Phonon modes in spontaneously ordered $GaInP_2$ studied by micro-Raman scattering measurements

Hyeonsik M. Cheong, F. Alsina, A. Mascarenhas, J. F. Geisz, and J. M. Olson
National Renewable Energy Laboratory, 1617 Cole Boulevard, Golden, Colorado 80401
(Received 9 December 1996; revised manuscript received 1 April 1997)

We have performed micro-Raman-scattering experiments on ordered $GaInP_2$ alloy samples in three different geometries where the phonon wave vector is either parallel or perpendicular to the ordering axis of the crystal. By comparing results from the (111) backscattering and right-angle scattering measurements with the C_{3v} symmetry of the crystal, we found that the recently discovered peaks at 205 and 354 cm^{-1} in the Raman spectra of ordered alloys are due to longitudinal-phonon modes with A_1 symmetry in these geometries. In the (110) backscattering geometry, selection-rule forbidden longitudinal-phonon modes appear in the Raman spectra measured in parallel polarizations. Possible mechanisms for this selection-rule violation are discussed. [S0163-1829(97)04128-3]

I. INTRODUCTION

Spontaneous $CuPt_B$-type long-range ordering in $GaInP_2$ has been a subject of intense study in recent years.[1] Depending on the growth conditions, $Ga_{0.52}In_{0.48}P$ (written as $GaInP_2$ for simplicity), grown lattice matched to a (001) GaAs substrate by organometallic vapor phase epitaxy (OMVPE), exhibits ordering of the cations on the group-III sublattice along [111] or [111], which are the two $[111]_B$ directions. The ordered alloys consist of monolayer superlattices of $Ga_{1+\eta}In_{1-\eta}P_2/Ga_{1-\eta}In_{1+\eta}P_2$ along the $[111]_B$ directions, where the order parameter η ranges from 0 to 1. When the ordering is single variant, i.e., the ordering occurs along only one of the two $[111]_B$ directions throughout the sample, this structure has trigonal symmetry with point group C_{3v}, while the random alloy of $GaInP_2$ has the cubic zinc-blende structure with point group T_d. The (001) backscattering Raman spectrum of the random alloy $GaInP_2$ consists of three major features:[2–10] a GaP-like longitudinal-optical-(LO-) phonon peak at ~380 cm^{-1}, an InP-like LO phonon peak at ~362 cm^{-1}, and a transverse-optical- (TO-) phonon band at ~330 cm^{-1}. In addition, it is believed that there is a TO-phonon peak between the two LO-phonon peaks.[11,12] In early Raman studies on the effects of ordering, no major change in the Raman spectrum was observed. With recent improvement in the sample qualities, however, there have been several reports[7–10] of major effects of ordering on the (001) Raman spectrum. Several effects are reported: (1) three extra peaks at ~60, ~205, and ~354 cm^{-1} appear in the Raman spectra of highly ordered samples; (2) the GaP-like LO-phonon peak blueshifts with increasing ordering by about 1 cm^{-1}; and (3) the peak at 354 cm^{-1} is enhanced when the excitation and the detection polarizations are aligned in the [110] direction while the peak at 205 cm^{-1} is enhanced when the polarizations are in the [110] direction. Hassine *et al.*,[9] report a larger blueshift (~4.5 cm^{-1}) and a 7-cm^{-1} splitting of the GaP LO peak, but this observation has not been reproduced by others. The extra peaks are often interpreted in terms of the C_{3v} symmetry of the ordered alloy.[7–9] However, since the $[111]_B$ ordering axis is neither parallel nor perpendicular to the phonon wave vector $\boldsymbol{q}$ in the [001] backscattering geometry, symmetry and polar characters of the modes are mixed, and therefore it is not possible to make definite assignments of the modes without *a priori* knowledge of the relative strengths of the LO-TO splitting and the A_1-E splitting. Lately, Mestres *et al.*[13] compared backscattering Raman spectra of (110) and (110) cleaved edges in an effort to find the correct phonon mode assignments for the new peaks. However, modes are again mixed in the (110) backscattering geometry and, as we will show later, the (110) backscattering geometry turns out to be problematic due to non-negligible forbidden scattering of the longitudinal modes. In this paper, we compare the results of micro-Raman-scattering experiments in three different geometries with $\boldsymbol{q}$ either parallel or perpendicular to the ordering axis to obtain the first definitive phonon mode assignments for the extra Raman peaks.

II. EXPERIMENT

We have performed micro-Raman measurements on several ordered $GaInP_2$ samples and the results for a typical sample presented in this paper were reproducible. A 10-μm-thick $GaInP_2$ epilayer was grown by OMVPE on a (001) semi-insulating (SI) GaAs substrate 6° misoriented toward $[111]_B$. A growth temperature of 680 °C and a growth rate of 5 μm/h were used. The SI substrate was used to quench the hot photoluminescence (PL) signal from the substrate in the right-angle scattering measurements. The substrate misorientation assures that the sample is single variant.[14] The exact orientation of the ordering axis was found by measuring the room-temperature photoluminescence on the two cleaved surfaces [(110) or (110)] of the sample and comparing the polarization of the PL.[15] The value of the order parameter η of the sample was estimated to be 0.46 ± 0.02 by comparing the low-temperature (10 K) PL and PL excitation spectra with theoretical calculations.[16–18]

We choose the two cleavage directions of the samples as $X=[110]$ and $Y=[110]$, and the growth direction as $Z=[001]$.[19] Since the sample is single variant, the principal axes of the crystal symmetry can be defined as the ordering

TABLE I. The C_{3v} Raman-scattering efficiency calculated with Eqs. (1) and (2) for the scattering geometries used in this work. We use the Porto's notation where $k_i(e_i,e_s)k_s$ refers to the scattering configuration in which k_i and k_s are the propagation directions of the incident and scattered photons, and e_i and e_s are the polarization directions of the incident and scattered photons, respectively. θ is the angle between the z' direction and the direction normal to the growth surface.

	A_1	$E_{x'}$	$E_{y'}$
$\overline{z'}(y',y')z'$, $\overline{z'}(x',x')z'$	a^2	c^2	0
$\overline{z'}(x',y')z'$, $\overline{z'}(y',x')z'$	0	0	c^2
$\overline{Z}(X,Z)\overline{X}$	$(a-b)^2\sin^2\theta\cos^2\theta$	$\{c\ \sin\theta\cos\theta+d(\cos^2\theta-\sin^2\theta)\}^2$	0
$\overline{Z}(Y,Y)\overline{X}$	a^2	c^2	0
$\overline{Z}(Y,Z)\overline{X}$	0	0	$(c\ \sin\theta-d\cos\theta)^2$
$\overline{Z}(X,Y)\overline{X}$	0	0	$(c\ \cos\theta+d\sin\theta)^2$
$y'(z',z')\overline{y'}$	b^2	0	0
$y'(x',x')\overline{y'}$	a^2	c^2	0
$y'(x',z')\overline{y'}$, $y'(z',x')\overline{y'}$	0	d^2	0

axis $z'=[\overline{1}11]$ and two axes perpendicular to it: $y'=Y=[110]$ and $x'=[112]$. The Raman spectra were taken in three geometries: backscattering on (110) and (111) surfaces, and right-angle scattering between the Z and X directions. For the (111) backscattering, a piece of the sample was polished normal to the [111] direction using 500-Å grit size colloidal silica. The backscattering measurements were performed in air through a 60× microscope objective using the 5145-Å line of an Ar ion laser as the excitation source. The power used was 1.5 mW and the spot size was $\leqslant 2$ μm, much smaller than the thickness of the epilayer, in order to ensure that the excitation laser light is fully contained in the correct surface of the $GaInP_2$ layer. The possible effect of local heating was checked by varying the excitation power, and no appreciable change in the Raman spectra was observed for powers up to ~5 mW. For the right-angle scattering, a titanium:sapphire laser tuned at 7400 Å, below the band-gap energy of $GaInP_2$, was used as the excitation. The laser power at the sample was 20 mW, focused to a spot size of ~50 μm in diameter. The focus spot was ~100 μm below the top edge of the (001) surface in order to prevent the diffracted laser light from reaching the top (110) surface. In both geometries, the signal was collected with the microscope objective, dispersed by a Spex 0.6-m triple spectrometer, and detected with a liquid-nitrogen-cooled high-resolution CCD detector array. The uncertainty in the Raman shift is estimated to be ± 2 cm^{-1}.

III. RESULTS AND DISCUSSION

In the C_{3v} symmetry, the three Raman-scattering tensors A_1, $E_{x'}$, and $E_{y'}$ that represent vibrations along z', x', and y', respectively, can be written as[20]

$$\begin{pmatrix} a & 0 & 0 \\ 0 & a & 0 \\ 0 & 0 & b \end{pmatrix}, \quad \begin{pmatrix} c & 0 & d \\ 0 & -c & 0 \\ d & 0 & 0 \end{pmatrix}, \quad \begin{pmatrix} 0 & -c & 0 \\ -c & 0 & d \\ 0 & d & 0 \end{pmatrix}. \tag{1}$$

The Raman-scattering efficiency can be written as

$$S \propto |\mathbf{e}_i R \mathbf{e}_s|^2, \tag{2}$$

where $\mathbf{e}_i$ and $\mathbf{e}_s$ are the unit vectors along the polarizations of excitation and scattered light, respectively, and R is the tensor for a particular mode. Table I summarizes the values of $|\mathbf{e}_i R \mathbf{e}_s|^2$ for the scattering geometries used in this work.

A. $(\overline{1}11)$ backscattering

In the backscattering geometry on the $(\overline{1}11)$ surface, $\boldsymbol{q}$ is along the z' direction, and therefore the A_1 tensor represents longitudinal modes and the $E_{x'}$ and $E_{y'}$ tensors represent transverse modes. Then, according to Table I, both longitudinal and transverse modes are allowed in parallel polarizations [$\overline{z'}(x',x')z'$ or $\overline{z'}(y',y')z'$], while only transverse modes are allowed in crossed polarizations [$\overline{z'}(x',y')z'$ or $\overline{z'}(y',x')z'$]. Figure 1 shows Raman spectra taken in this geometry for the four polarization configurations. Only the TO-phonon peak at 328 cm^{-1} appears strongly in the crossed polarizations, while the InP- and GaP-like LO-phonon peaks and the new peak at ~205 cm^{-1} also appear in the parallel polarizations. This is consistent with the previous interpretation[7,9,10] of the 205-cm^{-1} peak as a folded longitudinal-acoustic-phonon mode with A_1 symmetry. The extra peak at 354 cm^{-1} is not resolved in any of these spectra. This is also consistent with the (001) backscattering result where this peak is strong and clearly resolved only when the polarization has a z' component. In the current geometry, the polarization has no z' component. In the crossed polarizations, weak features appear at the frequencies of the LO phonons. These nominally forbidden peaks appear weakly because $\boldsymbol{q}$ has some component orthogonal to z' due to the large angle of incidence of the micro-Raman optics.

B. Right-angle scattering

In right-angle scattering where the excitation is in the $\overline{Z}$ direction and the detection in the X direction, $\boldsymbol{q}$ is at 45° relative to the Z direction. For a sample grown on a 6° misoriented substrate, the angle between the z' and Z axes is 48.7°. Therefore, in this geometry it is a good approximation to assume that $\boldsymbol{q}$ is parallel to z', and as in (111) backscatter-

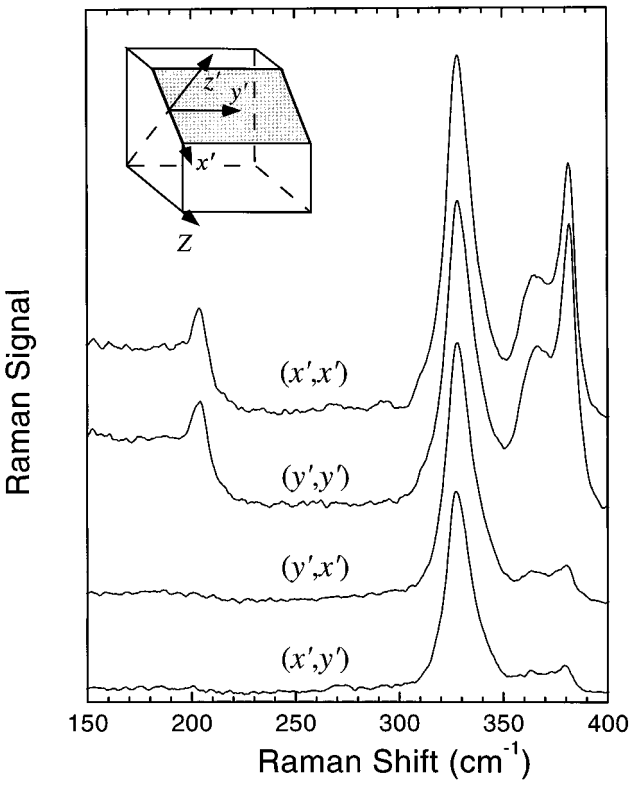

FIG. 1. Raman spectra of ordered $GaInP_2$ taken in the $(\bar{1}\bar{1}\bar{1})$ backscattering geometry in four different polarization configurations (e_i, e_s), where e_i and e_s are the polarization directions of the incident and scattered photons, respectively. The inset shows the scattering geometry.

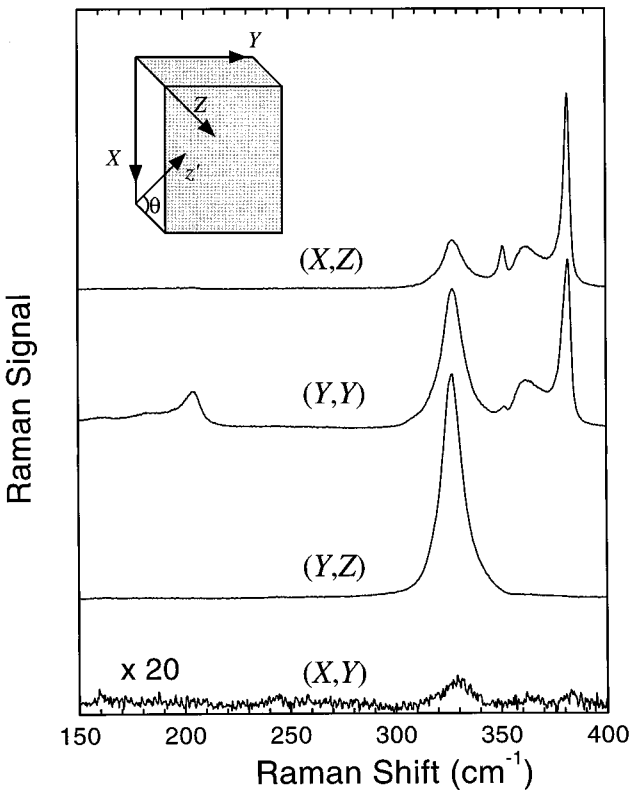

FIG. 2. Raman spectra taken in the right-angle scattering geometry where the excitation is in the Z direction and the detection in the X direction.

ing, the A_1 tensor represents longitudinal modes and the $E_{x'}$ and $E_{y'}$ tensors represent transverse modes. Table I lists the scattering efficiencies using $X=(\cos\theta,0,-\sin\theta)$, $Y=(0,1,0)$, and $Z=(\sin\theta,0,\cos\theta)$, where θ is the angle between the z' and Z axes.

Figure 2 shows four spectra taken for the four possible polarization configurations. In this geometry, the detected signal was a few orders of magnitude stronger than the backscattering case owing to the larger interaction volume. In the $Z(X,Y)X$ configuration, a very weak signal was detected for the TO-phonon peak at 328 cm^{-1}. This implies, according to Table I, that $c\cong -d\ \tan\theta\approx -d$ $(\theta\approx 45°)$ for this mode. In the $Z(Y,Z)X$ configuration, only the TO-phonon peak is detected as expected. Here, unlike the case of the (111) backscattering, no signal from the forbidden LO-phonon peaks was detected. This is due to the difference in the geometry of the optical setup; unlike the backscattering geometry, the excitation beam is almost perfectly parallel to the Z direction, and the microscope optics preferentially collect scattered photons nearly parallel to the X direction due to the high index of refraction of the material and the ~ 100-μm distance between the incident-beam path and the top (110) surface of the sample. It should also be noted that there is no indication of a TO-phonon peak between 362 and 380 cm^{-1} in this spectrum. It has been suggested that a TO-phonon peak between the two LO peaks at 362 and 380 cm^{-1} is responsible for the reduction of the so-called valley-depth ratio in the (001) Raman spectra of ordered alloys.[7,9] However, our data show that even if there exists a TO mode in this frequency range, it is very weak and so its contribution to the (001) Raman spectra would be negligible.

In the $Z(X,Z)X$ and $Z(Y,Y)X$ configurations, both longitudinal and transverse modes are allowed, and the spectra show the extra peaks at $\sim$354 cm^{-1} and at $\sim$205 cm^{-1} in addition to the two LO-phonon peaks and the TO-phonon peak. This, together with the behavior of this mode in the $Z(Y,Z)X$ and the $Z(X,Y)X$ configurations, is consistent with the result of the (111) backscattering which assigned the 205-cm^{-1} peak as an A_1 longitudinal mode. The 354-cm^{-1} peak is also an A_1 mode, because if it were an $E_{x'}$ mode, it should be about 4 times stronger in the $Z(Y,Y)X$ configuration than in the $Z(X,Z)X$ configuration $(\sin\theta\approx\cos\theta\approx 1/\sqrt{2})$. By comparing the intensities of these peaks with Table I, we can estimate the relative magnitude of some of the tensor components of Eq. (1) for each mode. The 205-cm^{-1} mode is strong in the $Z(Y,Y)X$, $\overline{z'}(x',x')z'$, and $\overline{z'}(y',y')z'$ configurations and weak in the $Z(X,Z)X$ configuration. Therefore, we can deduce $|a-b|\ll 2|a|$ $(\theta\approx 45°)$, or equivalently, $a\approx b$ for this mode. The 354-cm^{-1} peak shows an opposite behavior, and therefore $|a-b|\gg 2|a|$ for this mode. We also note that the positions of the peaks in Figs. 1 and 2 are the same within experimental uncertainties as those in the (001) spectra, which means that the anisotropy of the force constant is rather small. In order to check the effect of resonance, the excitation energy was varied from 1.675 eV (7400 Å) to 1.785 eV (6946 Å) and the above results were consis-

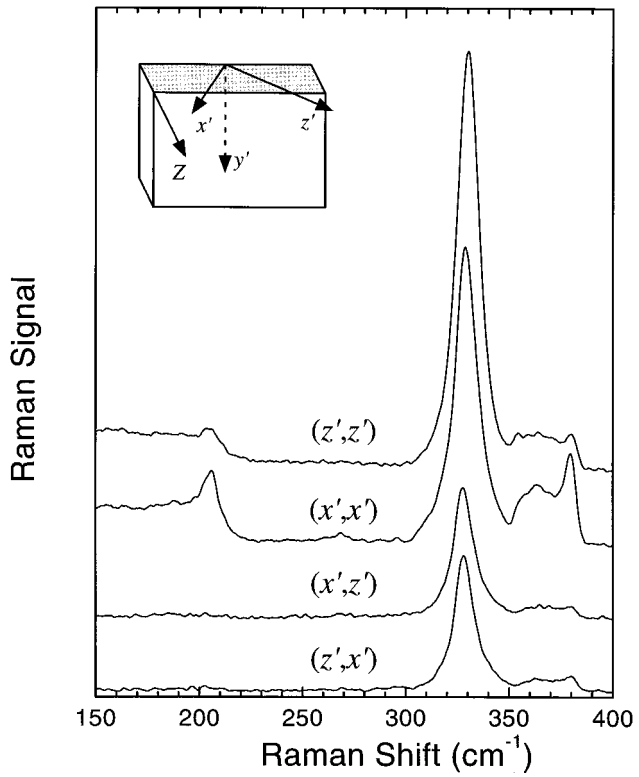

FIG. 3. Raman spectra taken in the (110) backscattering geometry. The forbidden LO modes are clearly seen in the parallel polarization configurations and are stronger in the $y'(x',x')\overline{y'}$ configuration than in the $y'(z',z')\overline{y'}$ configuration.

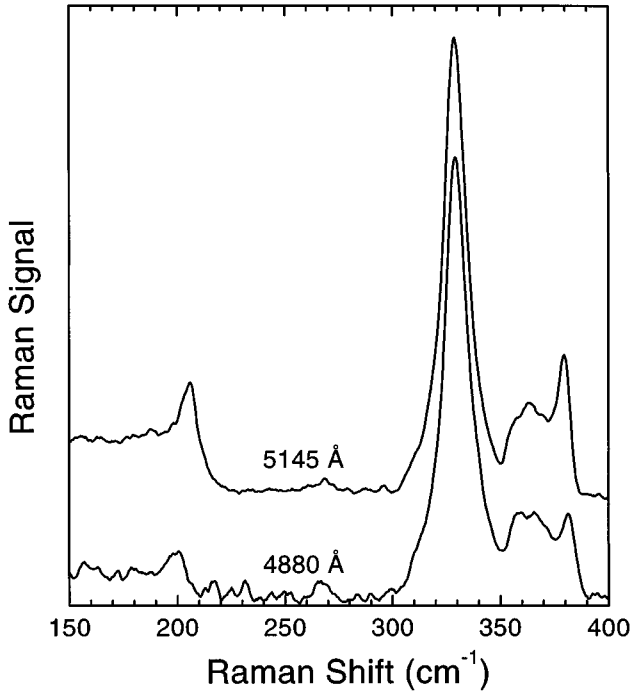

FIG. 4. Comparison of Raman spectra taken in the (110) backscattering geometry with 5145- and 4880-Å excitations. The forbidden LO modes at 360–385 are weaker in the spectrum for the 4880-Å excitation. The relative intensity of the 205-cm^{-1} peak is also lower for the 4880-Å excitation, which indicates that this peak is also due to a forbidden longitudinal mode.

tent throughout the excitation energy range. (The room-temperature band gap of the sample was ~1.81 eV.)

C. (110) backscattering

In the backscattering geometry from the (110) cleaved surface, $\boldsymbol{q}$ is along the y' direction; the $E_{y'}$ tensor represents longitudinal modes and the $E_{x'}$ and A_1 tensors represent transverse modes. Therefore, only transverse modes are allowed in any of the four polarization configurations according to Table I. Figure 3 shows Raman spectra taken in this geometry. The TO-phonon peak at 328 cm^{-1} is present in all four spectra as expected. In addition, the forbidden $E_{y'}$ symmetry LO-phonon peaks at 362 and 380 cm^{-1}, and the peak at 205 cm^{-1} are clearly observed in the parallel polarizations. Some signal from the forbidden modes is expected due to the geometry of the micro-Raman optics as discussed earlier for the case of the (111) backscattering. However, if the LO-phonon signal in these spectra is solely due to the geometry of the optical setup, the intensities of the forbidden LO peaks should be the same for the two parallel polarizations; for example, we observed a very weak signal from the forbidden LO-phonon mode for the GaAs substrate of this sample and its intensity did not depend on the direction of the polarizations. In this case, however, there is a clear directionality; the forbidden modes are much stronger for the $y'(x',x')\overline{y'}$ configuration than for the $y'(z',z')\overline{y'}$ configuration. This also rules out a breakdown of the translational symmetry due to random disorder as the cause of this selection-rule violation. Two possible mechanisms for this breakdown are $\boldsymbol{q}$-dependent Fröhlich interaction and Fröhlich interaction due to the electric field induced by surface charges.[21,22] Both these forbidden scattering mechanisms are dependent on the excitation energy with enhancement near the resonance with an interband transition. In our case, the excitation energy (2.41 eV) is not far from the interband transition between the spin-orbit valence band and the folded L band state (L'_{1c}), which has an energy of ~2.3 eV.[1] In order to check this possibility, we repeated the (110) backscattering measurements using the 4880-Å line (2.54 eV) as the excitation; the forbidden scattering should be weaker for the 4880-Å excitation. Figure 4 compares two Raman spectra taken in the $y'(x',x')\overline{y'}$ configuration under nominally identical conditions except for the excitation wavelength. The overall Raman signal was weaker for the 4880 Å probably due to a combination of some resonance effect and the fact that our spectroscopy system was optimized for the 5145-Å excitation. In Fig. 4, the spectra were normalized for the TO-phonon peak for comparison. It is seen that the relative intensity of the LO-phonon band at 360–385 cm^{-1} is significantly smaller for the 4880-Å excitation. A similar effect was observed for the $y'(z',z')\overline{y'}$ configuration. This is consistent with the above assumption that these peaks appear due to forbidden scattering. Also, since these forbidden scattering mechanisms reflect the symmetry of the crystal, the strength of the interactions would be different for different polarizations as we have observed. It should be pointed out that one would not observe selection-rule violations due to these forbidden scatterings in geometries with $\boldsymbol{q}\|z'$, because

in those cases, A_1 longitudinal modes are already selection-rule allowed when these Frölich interactions are allowed (parallel polarizations).

It is also seen in Fig. 4 that the relative intensity of the 205-cm^{-1} peak is much smaller for the 4880-Å excitation. This implies that this mode has similar characteristics as the GaP- and InP-like LO phonons at 360–385 cm^{-1}, which are $E_{y'}$ longitudinal modes. This contradicts the interpretation of Mestres *et al.*,[13] who interpreted this peak as an A_1 transverse mode in this geometry based on the assumption that the LO-TO splitting is very small for this mode. Since they used only the 5145-Å excitation and ignored the rather significant intensity of the LO-phonon band at 360–385 cm^{-1}, they assumed that the strong signal of the 205-cm^{-1} peak in this geometry was consistent with this being an allowed A_1 mode. However, our current data clearly indicate that this peak's behavior closely resembles those of the GaP- and InP-like LO phonons, which have $E_{y'}$ symmetry in this scattering geometry.

IV. CONCLUSIONS

We performed micro-Raman-scattering measurements on spontaneously ordered $GaInP_2$ samples in scattering geometries where the phonon wave vector $\boldsymbol{q}$ is either parallel or perpendicular to the ordering direction z', which is the uniaxial direction of the trigonal C_{3v} symmetry of the crystal. By comparing the selection rule and the results of the (111) backscattering and the right-angle scattering, where $\boldsymbol{q} \| z'$, we identified the extra peaks at 205 and 354 cm^{-1} as A_1 longitudinal modes. In (110) backscattering, we observed forbidden scattering of GaP- and InP-like LO phonons, and found that the 205-cm^{-1} mode also behaves like these LO phonons which are $E_{y'}$ longitudinal modes in this geometry.

ACKNOWLEDGMENTS

We thank C. Kramer and K. Jones for help with sample preparation. This work was supported by the Office of Energy Research (Material Science Division) of the Department of Energy under Contract No. DE-AC36-83-CH10093.

[1] For a review of recent progress in this field, see A. Zunger and S. Mahajan, in *Materials, Properties and Preparation,* edited by S. Mahajan, Handbook on Semiconductors, 2nd ed. (North-Holland, Amsterdam, 1994), Vol. 3B, p. 1399.

[2] T. Suzuki, A. Gomyo, S. Iijima, K. Kobayashi, S. Kawata, I. Hino, and T. Yuasa, Jpn. J. Appl. Phys. **27**, 2098 (1988).

[3] M. Kondow and S. Minagawa, J. Appl. Phys. **64**, 793 (1988).

[4] K. Sinha, A. Mascarenhas, G. S. Horner, R. G. Alonso, K. A. Bertness, and J. M. Olson, Phys. Rev. B **48**, 17 591 (1993).

[5] K. Sinha, A. Mascarenhas, G. S. Horne, K. A. Bertness, S. R. Kurtz, and J. M. Olson, Phys. Rev. B **50**, 7509 (1994).

[6] K. Uchida, P. Y. Yu, N. Noto, Z. Liliental-Weber, and E. R. Weber, Philos. Mag. B **70**, 453 (1994).

[7] F. Alsina, N. Mestres, J. Pascual, C. Geng, P. Ernst, and F. Scholz, Phys. Rev. B **53**, 12 994 (1996).

[8] A. M. Mintairov and V. G. Melehin, Semicond. Sci. Technol. **11**, 904 (1996).

[9] A. Hassine, J. Sapriel, P. Le Berre, M. A. Di Forte-Poisson, F. Alexandre, and M. Quillec, Phys. Rev. B **54**, 2728 (1996).

[10] H. M. Cheong, A. Mascarenhas, P. Ernst, and C. Geng, preceding paper, Phys. Rev. B **56**, 1882 (1997).

[11] B. Jusserand and S. Slempkes, Solid State Commun. **49**, 95 (1984).

[12] T. Kato, T. Matsumoto, and T. Ishida, Jpn. J. Appl. Phys. 1 **27**, 983 (1988).

[13] N. Mestres, F. Alsina, J. Pascual, J. M. Bluet, J. Camassel, C. Geng, and F. Scholz, Phys. Rev. B **54**, 17 754 (1996).

[14] P. Bellon, J. P. Chevalier, E. Augarde, J. P. André, and G. P. Martin, J. Appl. Phys. **66**, 2388 (1989).

[15] G. S. Horner, A. Mascarenhas, R. G. Alonso, D. J. Friedman, K. Sinha, K. A. Bertness, J. G. Zhu, and J. M. Olson, Phys. Rev. B **48**, 4944 (1993).

[16] P. Ernst, C. Geng, F. Scholz, H. Schweizer, Y. Zhang, and A. Mascarenhas, Appl. Phys. Lett. **67**, 2347 (1995).

[17] S.-H. Wei, D. B. Laks, and A. Zunger, Appl. Phys. Lett. **62**, 1937 (1993).

[18] K. A. Mäder and A. Zunger, Phys. Rev. B **51**, 10 462 (1995).

[19] Due to the substrate misorientation, the growth direction is not exactly [001] but tilted by 6°. For simplicity, we denote the growth direction as $Z=[001]$ in this paper.

[20] W. Hayes and R. Loudon, *Scattering of Light by Crystals* (Wiley, New York, 1978).

[21] Our OMVPE-grown $GaInP_2$ samples are moderately *n* type with a background doping density of $\sim 10^{17}$ cm^{-3}.

[22] F. Schäffler and G. Abstreiter, Phys. Rev. B **34**, 4017 (1986).